nature neuroscience

Inhibitory synapses in the developing auditory system are glutamatergic

Deda C Gillespie[1], Gunsoo Kim[1,2] & Karl Kandler[1,2]

Activity-dependent synapse refinement is crucial for the formation of precise excitatory and inhibitory neuronal circuits. Whereas the mechanisms that guide refinement of excitatory circuits are becoming increasingly clear, the mechanisms guiding inhibitory circuits have remained obscure. In the lateral superior olive (LSO), a nucleus in the mammalian sound localization system that receives inhibitory input from the medial nucleus of the trapezoid body (MNTB), specific elimination and strengthening of synapses that are both GABAergic and glycinergic (GABA/glycinergic synapses) is essential for the formation of a precise tonotopic map. We provide evidence that immature GABA/glycinergic synapses in the rat LSO also release the excitatory neurotransmitter glutamate, which activates postsynaptic NMDA receptors (NMDARs). Immunohistochemical studies demonstrate synaptic colocalization of the vesicular glutamate transporter 3 with the vesicular GABA transporter, indicating that GABA, glycine and glutamate are released from single MNTB terminals. Glutamatergic transmission at MNTB-LSO synapses is most prominent during the period of synapse elimination. Synapse-specific activation of NMDARs by glutamate release at GABAergic and glycinergic synapses could be important in activity-dependent refinement of inhibitory circuits.

In the developing brain, activity-dependent refinement has a central role in establishing precise neuronal circuits[1]. Although the refinement of excitatory circuits has been extensively studied, the rules and mechanisms by which inhibitory circuits are refined remain poorly understood. Numerous studies have shown developmental and activity-dependent modifications of inhibitory circuitry that include changes in receptor and synaptic properties and in overall expression of GABAergic markers[2–7]. However, the complexity of the majority of inhibitory networks in the vertebrate brain has hindered progress in understanding how these molecular and synaptic changes translate into plasticity at the level of functionally-defined inhibitory circuits.

Reorganization of specific inhibitory circuits has been well documented in the developing auditory system[8]. The LSO is a binaural auditory brainstem nucleus involved in sound localization. In order to compute interaural intensity differences, the LSO integrates excitatory input from the cochlear nucleus with inhibitory input from the MNTB, whose neurons are both GABAergic and glycinergic at the initial stages in development but become glycinergic in early postnatal life[9–12]. Activity-dependent refinement of MNTB-LSO connections is necessary for the formation of a precise inhibitory tonotopic map. In the MNTB-LSO pathway, tonotopic precision is achieved through an early phase of functional refinement that occurs before the onset of hearing[13] and a later phase of structural reorganization that occurs after hearing onset[14]. The pre-hearing phase of functional refinement is characterized by elimination of most of the initial GABA/glycinergic inputs and by strengthening of the remaining inputs[13]. These processes take place at an age when MNTB-LSO synapses are primarily GABAergic rather than glycinergic[11,12] and when GABA and glycine are depolarizing rather than hyperpolarizing[15]. Although functional refinement occurs before hearing onset and thus without sound-evoked neuronal activity, it clearly depends on cochlea-generated spontaneous activity, as tonotopic precision is impaired by neonatal cochlea ablation or by pharmacological blockade of glycine receptors[14].

Here we show that activation of the GABA/glycinergic MNTB-LSO pathway in slices from neonatal rats elicits a glutamate response in postsynaptic LSO neurons. This current is not due to glycine spillover[16] but instead reflects glutamate release from MNTB terminals. Our minimal stimulation experiments indicated that glutamate, GABA and glycine are released by single MNTB axons, and immunohistochemical evidence suggested that all three neurotransmitters are released from single synaptic terminals. Glutamate transmission was age dependent and was most prominent during the early period of functional refinement. The transient glutamatergic phenotype of the immature GABA/glycinergic MNTB-LSO pathway may provide synapse-specific activation of MNTB-type glutamate receptors and thus could represent a previously unknown mechanism for the developmental reorganization of this inhibitory circuit.

RESULTS

MNTB stimulation elicits glutamatergic responses in LSO

Whole-cell voltage-clamp recordings were made from LSO neurons in acute brain slices from postnatal day 1–12 (P1–12) rats in Mg^{2+}-free solution. Electrical stimulation of the MNTB produced synaptic currents that were inwardly directed owing to the high

[1]Department of Neurobiology and [2]Center for Neurological Basis of Cognition, University of Pittsburgh School of Medicine, W1412 Biomedical Science Tower, 3500 Terrace St., Pittsburgh, Pennsylvania 15261, USA. Correspondence should be addressed to K.K. (kkarl@pitt.edu).

Published online 30 January 2005; doi:10.1038/nn1397

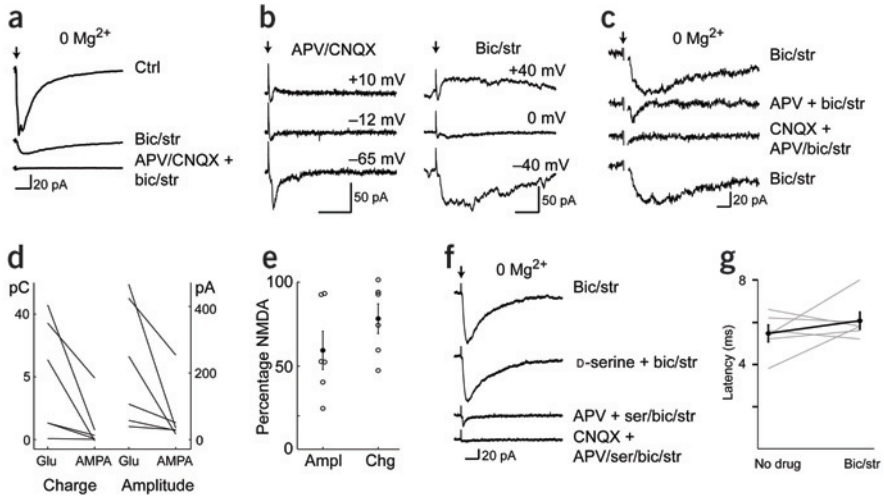

Figure 1 Electrical stimulation of the MNTB causes release of glutamate at synapses in the LSO. (**a**) In Mg^{2+}-free ACSF, MNTB stimulation caused a large, slowly decaying response that was reduced but not abolished by the $GABA_AR$ antagonist bicuculline (10 μM) and the glycine receptor antagonist strychnine (1 μM). The residual response was abolished by the addition of ionotropic glutamate receptor antagonists D,L-APV (100 μM) and CNQX (5 μM). P5 slice; traces shown are average of 20 responses. Scale bars: 20 pA, 50 ms. Black arrow: stimulus artifact. Unless otherwise indicated, holding potentials were approximately –60 mV. (**b**) Isolated GABA/glycine and glutamate currents in LSO neuron in Mg^{2+}-free ACSF, in P2 slice. Application of D-APV (50 μM) and CNQX (5 μM) isolated a GABA/glycine current that reversed near the calculated Cl^- reversal potential of –14 mV (left). Washout of APV and CNQX isolated a glutamate current that reversed at +10 mV (right). Scale bars: 50 pA, 50 ms. (**c**) Recordings from LSO neuron in Mg^{2+}-free ACSF with bicuculline (10 μM) and strychnine (10 μM). APV removed the slowly decaying component, leaving a CNQX-sensitive component. Scale bars: 20 pA, 10 ms. (**d**) For six cells in which AMPA and NMDA currents were pharmacologically separated, amount of glutamate current charge (left) and amplitude (right) mediated by NMDARs. (**e**) Percentage of glutamate peak amplitude (left) or charge (right) mediated by NMDARs. Filled circles: averages ± s.e.m. (**f**) Recording in Mg^{2+}-free ACSF in a P7 slice. Saturation of the glycine site by perfusion of D-serine (200 μM) for 5 min did not occlude the glutamatergic MNTB response, which is composed of both NMDAR and AMPAR components. Scale bars: 20 pA, 50 ms. (**g**) Response latencies for mixed and isolated glutamatergic currents recorded in Mg^{2+}-free ACSF were not significantly different ($P = 0.3$, paired t-test, $n = 6$).

internal chloride concentration of the pipette solution (**Fig. 1a**). Despite the well-documented GABA/glycinergic nature of MNTB neurons[17], these currents were only partially blocked by the $GABA_A$ and glycine receptor antagonists bicuculline (10–20 μM) and strychnine (1–30 μM) (31/42 cells, P1–P12). The current remaining after application of bicuculline or strychnine reversed at positive membrane potentials ($V_{rev} = +5.0 \pm 4.6$ mV, $n = 4$), in contrast to pure GABA/glycine currents, which reversed at -14.8 ± 4.8 mV ($n = 4$ cells), close to the calculated reversal potential for chloride (–14 mV) (**Fig. 1b**). In all cases ($n = 31$), the bicuculline- and strychnine-insensitive current was blocked by the glutamate receptor antagonists APV (50 μM D-APV or 100 μM D,L-APV), CNQX (5 μM), or both, indicating that it was mediated by glutamate receptors.

Glutamate acts on NMDA receptors

MNTB-elicited glutamate responses had a long decay time course suggestive of an NMDAR-mediated component. Consistent with this, the NMDAR antagonist D-APV (50 μM, $n = 6$) abolished a large portion of the current, leaving behind a fast, rapidly decaying component that was sensitive to the AMPA and kainate receptor (AMPA/KA-R) antagonist CNQX (5 μM; $n = 5$ cells) (**Fig. 1c**). On average, NMDARs contributed over three-quarters of the glutamatergic synaptic charge and over half of the peak current (80.8 ± 7.9% charge, or 64.2 ± 10.9% peak current, $n = 7$) (**Fig. 1d,e**).

In the spinal cord, glycinergic synapses can activate NMDARs through the spillover of glycine onto the glycine site of the NMDAR[16], a mechanism that could also be responsible for the apparent glutamatergic response we observed in the MNTB-LSO pathway. To test this possibility, we saturated the NMDAR glycine site with high concentrations of the agonist D-serine (100–500 μM) in an attempt to occlude the response to synaptically released glycine. D-Serine had little effect on MNTB-elicited glutamate currents (**Fig. 1f**; 7.0 ± 9.0% reduction in peak amplitude, $n = 8$ cells), indicating that the majority of NMDARs were activated by glutamate, not by glycine. This result, together with the fact that most responses included an AMPAR-mediated component that could not have been activated by glycine (**Fig. 1c–f**), strongly suggests that MNTB fibers release glutamate or another excitatory neurotransmitter such as aspartate that is capable of activating ionotropic glutamate receptors. The sensitivity of the glutamate response to APV (**Fig. 1c–f**), together with the failure of D-serine to block the response, further excludes the possibility that the current resulted from activation of NR3-containing excitatory glycine receptors[18], lending support to the idea that glutamate is released by MNTB fibers.

Glutamate is released from MNTB neurons

It is possible that this glutamate release stems from activation of a disynaptic pathway between the MNTB and the LSO, as GABA and glycine are depolarizing and excitatory at this age[19] and thus could activate glutamatergic neurons that project to the LSO. This would have to be a pathway whose glutamatergic neurons were excited independently of $GABA_A$ and glycine receptor activation, as these receptors were blocked here. In addition, if there were a disynaptic pathway, we would expect a latency difference between monosynaptic GABA/glycine currents and disynaptic glutamate currents. However, the small difference in response latencies for the isolated glutamate current and the mixed current (**Fig. 1f,g**) (0.6 ± 0.5 ms at room temperature, $P = 0.3$, paired t-test, $n = 6$) argues against a disynaptic MNTB-LSO pathway. This is in agreement with previous anatomical and physiological studies[13,20] that did not find disynaptic connections from the MNTB to the LSO. The small latency differences we observed at room temperature may instead reflect release of GABA/glycine and glutamate from distinct presynaptic vesicular pools or differences in the spatial distribution of postsynaptic receptors (for example, extra- versus perisynaptic) .

Previous studies *in vivo* and *in vitro* have demonstrated that in the adult, the MNTB-LSO pathway is purely glycinergic, and that during development it is GABAergic[5,9–12] as well. We were therefore concerned that the glutamatergic responses might have resulted from electrical stimulation of unknown glutamatergic fibers running near or through the MNTB. To test this possibility, we used focal photolysis of caged glutamate ($n = 9$ cells in 7 slices, P2–5) to activate specifically the somata and dendrites of MNTB neurons and to avoid stimulation of *en passant* axons (**Fig. 2**). Glutamate uncaging in the MNTB in the presence of bicuculline (10 μM) and strychnine (1–10 μM) still elicited a synaptic current

in LSO neurons that reversed at positive membrane potentials and was blocked by APV (**Fig. 2d**). These glutamatergic synaptic responses were very sensitive to the mediolateral location of the uncaging site within the MNTB (**Fig. 2a–c**). This reflects the topographic organization of the MNTB-LSO pathway and the very focal activation of the MNTB neurons around the uncaging site, making it very unlikely that neurons outside the MNTB were activated. These results indicate that immature MNTB neurons release glutamate in the LSO.

We next addressed the question of whether glutamate, on the one hand, and GABA and glycine, on the other, are released from distinct populations of MNTB neurons or from the same MNTB fibers (**Fig. 3a**). In these experiments, we used minimal stimulation techniques[13,21] and recorded in physiological Mg^{2+} conditions to minimize background noise caused by spontaneous NMDAR activation. In brain slices from P4–P7 rats, one-third of all presumptive single fibers (4 of 12 single-fiber recordings made on 12 cells in response to minimal stimulation) elicited a synaptic current (21.47 ± 6.55 pA) that persisted in the combined presence of bicuculline (10 μM) and strychnine (1 μM) (**Fig. 3b**,**c**) but was blocked by CNQX (5 μM) and D,L-APV (100 μM) (n = 3; data not shown). As was the case with multifiber stimulation, single-fiber glutamate currents had slightly, but statistically significantly, longer response latencies than mixed currents (0.175 ± 0.025 ms later, $P \leq 0.01$). These data, together with previous results[11], support the idea that individual MNTB fibers can release three neurotransmitters: glutamate, GABA and glycine.

Developmental profile

Because of the importance of NMDARs in the development and plasticity of excitatory and inhibitory neuronal circuits[22–24], we determined the developmental profile of glutamatergic transmission at MNTB-LSO synapses. In brain slices from P1–P8 rats, 96% of LSO neurons (25 of 26 cells) showed MNTB-elicited glutamatergic responses, whereas in slices from P9–P12 rats, this fraction was only 31% (4 of 13 cells) (**Fig. 4**). Notably, the period during which glutamatergic transmission was encountered most frequently coincides with the period during which GABA and glycine are also depolarizing in the LSO and during which MNTB-LSO synapses are undergoing functional refinement[13–15,25].

MNTB terminals contain both GABA and glutamate vesicles

We next asked whether markers of both glutamate and GABA/glycine terminals were expressed together in terminals in the LSO, as would be expected if glutamate release indeed is involved in synapse-specific refinement. We addressed this question by using the glutamate and GABA/glycine vesicular transporters, which are specific for their respective neurotransmitters and thus determine synaptic vesicle content[26], as markers. In the LSO, immunolabeling for the vesicular glutamate transporters VGLUT1 and VGLUT3 (n = 6 rats, P4–14) was so intense that the characteristic S-shaped LSO was instantly recognizable (**Fig. 5a**,**b**). VGLUT3 label in the LSO formed clusters (<1 μm) presumably representing synaptic terminals, as indicated by their immunoreactivity for the synaptic protein SV2 (n = 3 rats, **Fig. 5c**). Many of these VGLUT3-immunopositive clusters were also immunopositive for VGAT (**Fig. 5d**, n = 3 rats, Pearson's correlation coefficient = 0.22, control = 0.02). In triple labeling experiments, clusters labeled for both VGLUT3 and VGAT were also positive for SV2 (**Fig. 5e**,**f**), indicating that VGLUT3 and VGAT were present together in the same presynaptic terminals. In contrast, VGLUT1, which also was strongly expressed in the LSO, did not colocalize with VGAT (**Fig. 5g**), although it did colocalize with VGLUT2 (**Fig. 5h**).

Although the MNTB provides the principal inhibitory input to the LSO, other potential GABA/glycinergic inputs from the ventral nucleus of the trapezoid body have been described[5,17]. The clear labeling of most MNTB cell bodies not only for VGAT, as is expected from their GABA/glycinergic phenotype[27,28], but also for VGLUT3 makes it likely that most VGAT- and VGLUT3-positive terminals in the LSO are axon terminals from the MNTB (**Fig. 6a**, n = 6 rats, P4–14). To pursue this further, we filled individual MNTB cells (**Fig. 6b**,**c**) in acute brain slices (8 cells, 4 rats) and subsequently processed for SV2 and VGLUT3 immunoreactivity. SV2-positive presynaptic MNTB terminals were also VGLUT3 immunopositive (**Fig. 6d**,**e**), suggesting that individual MNTB terminals can contain glutamatergic as well as GABA/glycinergic vesicles, or perhaps even mixed glutamate/GABA/glycinergic synaptic vesicles.

DISCUSSION

Here we have presented physiological and anatomical evidence that developing GABA/glycinergic synapses also release glutamate. To our

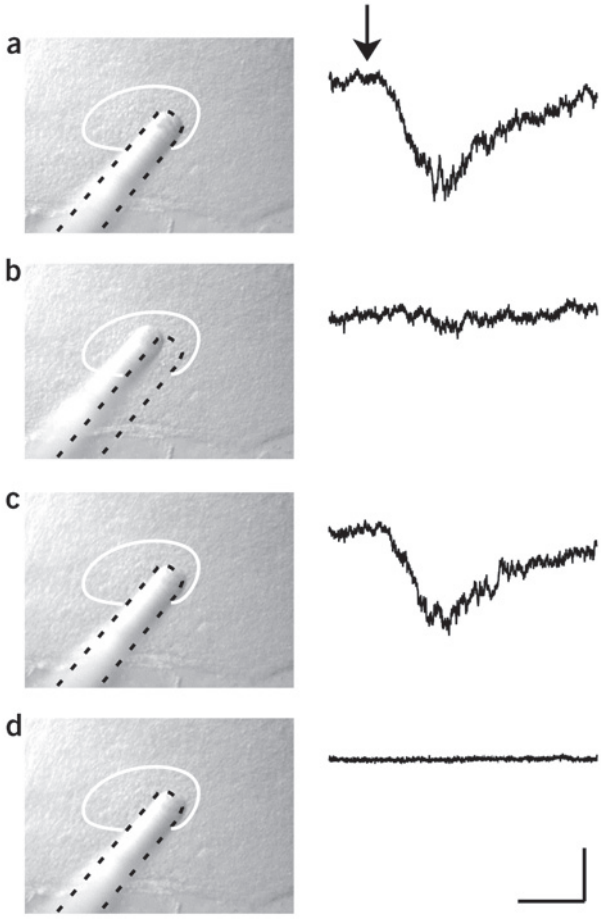

Figure 2 The glutamatergic response arises from cell bodies of the MNTB. (**a**–**d**) Position of optical fiber for glutamate uncaging is shown in left column (MNTB outlined in solid white; initial position of optical fiber outlined with dashed black line) and corresponding postsynaptic response in LSO neuron is shown in right column. Traces (average of three stimulations) are presented in order of acquisition. Focal application of glutamate in the MNTB produced an inward current (**a**) in an LSO neuron ~500 μm away. Uncaging at a nearby site (**b**) within the MNTB did not elicit a response, though it could subsequently elicit a response at the original site (**c**). Finally, D-APV (50 μM) bath application abolished the LSO response (**d**). Bicuculline (10 μM) and strychnine (10 μM) were present throughout. P4 slice. Scale bars: 20 pA, 100 ms.

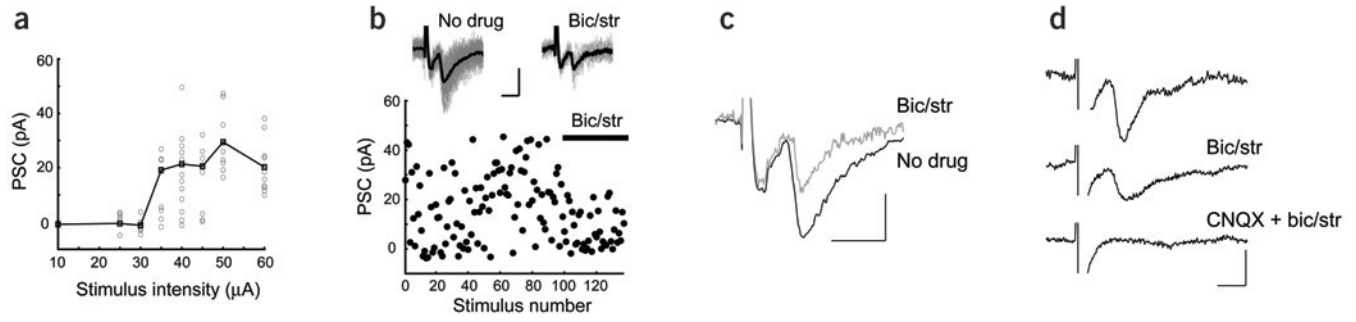

Figure 3 Minimal stimulation in a P7 LSO neuron in normal ACSF elicits a mixed GABA/glycine and glutamate response. (**a**) Input/output relationship in the absence of $GABA_A$/glycine receptor antagonists. (**b**) Current amplitudes recorded in response to minimal stimulation (failure rate 39% for this cell). Insets: individual (gray) and average (black) successful responses in no-drug and bicuculline + strychnine conditions. Scale bars: 20 pA, 5 ms. (**c**) Average mixed current (black trace, 25.9 pA) and isolated glutamate current (gray trace, 15.6 pA) responses to minimal stimulation. Scale bars: 10 pA, 5 ms. (**d**) Average single-fiber mixed response (top trace) with no drugs, isolated glutamate response (middle trace), and remaining response after application of CNQX (bottom trace). Responses were recorded in normal ACSF at holding potentials of –60 mV. **a**–**c**, P7 neuron; **d**, P6 neuron.

knowledge, this constitutes the first description of glutamate release at a GABA/glycinergic synapse. Previous studies have reported release of two fast-acting neurotransmitters by individual neurons, including GABA release from glutamatergic mossy fibers in young or kindled hippocampus[29–33]. The release of the three classical small amino acid neurotransmitters, with seemingly opposing postsynaptic functions, represents the most extreme example of multiple neurotransmitter release. Our results also provide a functional explanation for the long puzzling but neglected findings of high levels of glutamate immunoreactivity in MNTB cells[34] and of immunoreactivity for both glycine and glutamate in axon terminals in the LSO[35].

Why has glutamatergic transmission not been previously described in this well-studied pathway? In addition to inputs from the MNTB, LSO neurons receive prominent glutamatergic inputs from other sources[17]. Consequently, the glutamatergic currents that have occasionally been observed after MNTB stimulation have been seen as resulting from activity in these other glutamatergic fibers and hence have been ignored or pharmacologically blocked[11,36]. In addition, most of the MNTB-elicited glutamate response is mediated by NMDARs, which, as elsewhere, are magnesium sensitive in the LSO[37]. Therefore, in voltage-clamp recordings at normal resting membrane potentials and at physiological Mg^{2+} concentrations, NMDARs will remain blocked. In current-clamp recordings, relief of Mg^{2+} block is likely to depend on depolarizations by GABA or glycine[15,36,38], so pharmacological blockade of GABA and glycine channels would also prevent activation of NMDARs.

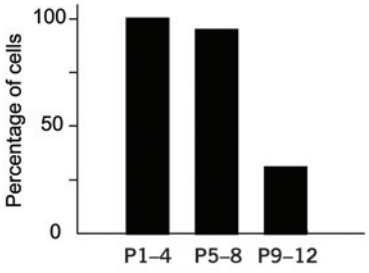

Figure 4 Developmental profile of the glutamatergic response. For each of three age groups, the percentage of LSO cells recorded that showed a glutamatergic response to MNTB stimulation is shown. (n = 9, 19 and 13 cells for groups P1–4, P5–8 and P9–12, respectively, χ^2 $P <$ 0.001). Age groups match published chloride reversal potentials in LSO neurons of –47, –58 and –82 mV (ref. 25).

Our immunolabeling results demonstrate that VGAT-positive MNTB neurons and terminals also express the vesicular glutamate transporter VGLUT3 but do not express VGLUT1. This suggests that glutamate release from GABA/glycinergic MNTB terminals is mediated by VGLUT3, whereas glutamate release from cochlea nucleus axon terminals is mediated by VGLUT1 and VGLUT2 or by VGLUT2 alone. VGLUT3 was recently identified by homology to VGLUT1 and VGLUT2, the vesicular glutamate transporters most commonly associated with glutamatergic terminals[39–42]. The role of VGLUT3 in the nervous system is still unknown, as this transporter is structurally and functionally similar to VGLUT1 and VGLUT2 yet is expressed in terminals of cholinergic, serotonergic, GABAergic and glycinergic neurons[42]. It has been proposed that VGLUT3 supports glutamate release from these 'non-glutamatergic' neurons, and VGLUT3 has been reported to mediate release of glutamate from dendrites[43]. Dendritic glutamate release from LSO neurons is unlikely here, as it would have to be triggered by a signal other than activation of $GABA_A$ and glycine receptors, which were blocked in our experiments. In addition, dendritic release would have added an apparent synaptic delay, which was not observed, to the glutamate response. Glutamate release from VGLUT3-positive GABA/glycinergic terminals thus provides the first functional support, albeit only correlative, for the hypothesis that VGLUT3 enables release of glutamate from 'non-glutamatergic' presynaptic terminals.

Glutamatergic neurotransmission in this pathway was most prevalent during the first postnatal week. It is unlikely that a switch in neonatal glycine receptor subtypes[44], accompanied by decreased strychnine affinity, could alone account for our results, as (i) we increased the strychnine concentration tenfold in some cases to ensure that glycine receptors were blocked and (ii) the residual current showed the reversal potential and pharmacology expected of a glutamate, not a glycine, current. We do not currently know what signals and mechanisms initiate and mediate the closure of this glutamatergic period. However, it is intriguing that downregulation of glutamatergic transmission correlates with other fundamental changes at this synapse, some of which could be involved in closing the glutamatergic period. For example, at the end of the first postnatal week, the quality of MNTB-LSO synapses switches from depolarizing to hyperpolarizing[11,12,15,25]. As a consequence of this switch, these synapses lose their ability to increase postsynaptic calcium concentration, which in turn may influence the number or activity of postsynaptic glutamate receptors[45]. At the same time, the transmitter phenotype of MNTB neurons changes from predominantly

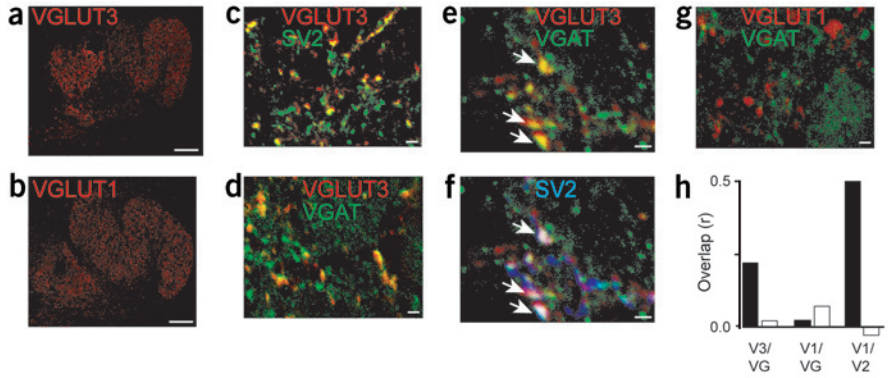

Figure 5 Immunostaining for vesicular transporters in the LSO. (**a**) VGLUT3 expression clearly identifies the S-shaped LSO of P5 rat brain, and also brightly labels the superior paraolivary nucleus just medial to the LSO. (**b**) VGLUT1 expression in the LSO of P5 rat clearly identifies the S-shaped LSO and the medial superior olive. Scale bars: 100 µm. Dorsal is up and lateral to the right in both frames. (**c**) VGLUT3 (red) and SV2 (green) immunoreactivity colocalize (yellow) in the LSO. (**d**) VGLUT3 clusters (red) and VGAT clusters (green) colocalize (yellow) in presumptive terminals in the LSO. (**e**) Two-channel image of triple-labeled section shows colocalized (yellow) VGLUT3 clusters (red) and VGAT clusters (green). (**f**) Addition of the SV2 channel (blue) to the image shows that these VGLUT3-VGAT colocalized clusters are in presynaptic terminals, as indicated by their colocalization (white) with SV2. Scale bars in **e**,**f**: 1 µm. (**g**) VGLUT1 does not colocalize with VGAT, as indicated by the distinct green and red, and the absence of yellow, label. Scale bars in **c**,**d**,**g**: 2 µm. Images **d** and **g** are from adjacent sections of the same P5 LSO. (**h**) Overlap coefficient (Pearson's *r*) for different immunolabeled protein pairs (black bars). As a random colocalization control using two images with the same spatial statistics, correlation coefficients were recalculated for the same image pairs after reflecting the green channel across the vertical or horizontal axis (white bars indicate average correlation coefficients for image pairs with the green channel reflected across each axis).

GABAergic to predominantly glycinergic, and MNTB inputs consequently activate different classes of postsynaptic receptors along with their associated downstream effectors. Finally, the apparent down-regulation of functional glutamate transmission could also reflect changes in presynaptic glutamate release or in glutamate uptake[46]. Future experiments addressing these possibilities will be necessary to understand potential interactions between early glutamatergic transmission and these changes in basic synaptic properties.

What is the role of glutamate release at GABA/glycinergic synapses? Glutamatergic transmission coincides with the period when MNTB-LSO connections are either eliminated or strengthened, which is crucial for tonotopic sharpening. NMDARs are pivotal in the development and plasticity of not only excitatory but also inhibitory synapses[23]. For example, at several GABAergic and glycinergic synapses, NMDAR-mediated calcium influx is required for the induction of long-term plasticity[47,48]. In immature hippocampal neurons, GABAergic synapses can activate NMDARs through the depolarizing action of GABA, which removes the Mg^{2+} block of NMDARs and allows activation of NMDARs by glutamate[38]. However, the source of glutamate at these GABAergic synapses has been an open question. Glutamate release at depolarizing GABA/glycinergic synapses provides a straightforward mechanism by which GABA/glycinergic inputs could gain access to activated NMDARs in a synapse-specific manner. This previously unknown mechanism for NMDAR activation by GABA/glycinergic synapses might mediate synapse-specific refinement and tonotopic sharpening during the development of this glycinergic map. It remains to be shown whether glutamate release at developing inhibitory synapses also occurs at other GABAergic or glycinergic synapses. However, in light of the VGLUT3 expression observed in a variety of GABA and glycinergic neurons[42], this seems a likely possibility.

Note added in proof: *While this paper was in press, a paper appeared (Boulland, J.L. et al., J. Comp. Neurol.* ***480****, 264–280, 2004) that demonstrated the transient expression of VGLUT in the SOC, supporting our finding that glutamate is an additional neurotransmitter in the SOC during an early postnatal period.*

METHODS

Electrophysiology. Experimental procedures were in accordance with US National Institutes of Health guidelines and were approved by the Institutional Animal Care and Use Committee at the University of Pittsburgh. Rats aged postnatal day 1–12 (P1–12) were deeply anesthetized with hypothermia or isofluorane, brains were removed in ice-cold artificial CSF (ACSF) with 1 mM kynurenic acid, and 300-µm-thick coronal slices were cut with a vibratome. Slices were allowed to recover for at least 1 h in an interface chamber before recording. Slices were transferred to a submersion-type chamber mounted on an upright microscope and perfused continuously with Mg^{2+}-free ACSF, containing (in mM), NaCl, 126; K_2SO_4, 1; KCl, 3; KH_2PO_4, 1.25; dextrose, 10; $NaHCO_3$, 26; and $CaCl_2$, 2. A 1-MΩ patch electrode filled with ACSF was placed in the MNTB for electrical stimulation. For photostimulation, *p*-hydroxyphenacylglutamate[49] (200 µM) was added to the ACSF. UV light pulses (50–100 ms) were delivered via an optical fiber (40 µm) placed directly above the MNTB to uncage glutamate focally. Electrodes (borosilicate glass, A-M Systems) were pulled to 1–4 MΩ and filled with a cesium gluconate solution containing (in mM) D-gluconic acid, 64; CsOH, 64; EGTA 11; CsCl, 56; $MgCl_2$, 1; $CaCl_2$, 1; HEPES, 10; and QX-314, 5). Stock

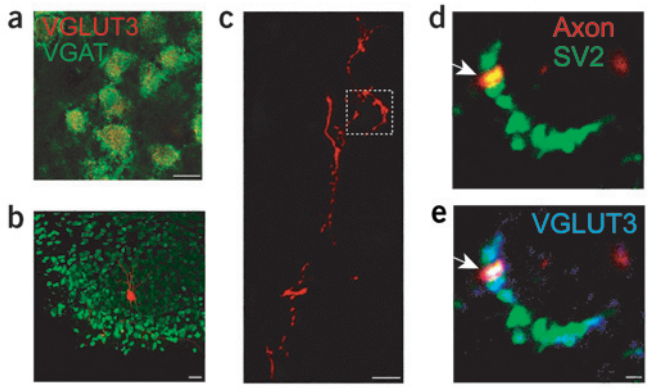

Figure 6 Immunostaining for vesicular transporters VGAT and VGLUT3 in cells of the MNTB. (**a**) MNTB cell bodies contain both VGAT (green) and VGLUT3 (red) immunoreactivity. Scale bar: 10 µm. (**b**) MNTB neuron filled with Alexa 568. Scale bar: 10µm. (**c**) Dye-filled MNTB axon collateral (red) in the LSO, compressed *z*-stack. Scale bar: 10 µm. (**d**) Two-channel image shows SV2-labeled (green) presynaptic terminals of identified MNTB axon (red; presynaptic terminals of this axon are thus yellow). Scale bar: 10 µm. (**e**) Three-channel image with VGLUT3 (blue) indicates the presence of VGLUT3 in identified MNTB presynaptic terminal. Scale bar: 1 µm.

solutions of bicuculline (Tocris), strychnine (Sigma), CNQX (Tocris) and/or D- or D,L-APV (Tocris) were diluted in ACSF for bath application. Whole-cell voltage clamp recordings were obtained from principal cells of the LSO visualized with gradient contrast optics (Luigs-Neumann). Signals were filtered at 2 kHz (Axon Instruments) and digitized at 5 kHz (custom LabView acquisition program). Offline analysis of acquired traces was performed with custom LabView and Matlab programs. Latencies, determined from averaged responses, were taken to be the point at which responses reached 20% of their peak amplitude. For minimal stimulation experiments, which were performed in normal Mg^{2+} ACSF (containing, in mM: NaCl, 126; $MgSO_4$, 1.3; KCl, 3; KH_2PO_4, 1.25; dextrose, 10; $NaHCO_3$, 26; and $CaCl_2$, 2), a stimulus-response relation was obtained and the first plateau was determined at stimulus intensities for which failure rate decreased without increasing the mean amplitude of successful responses (**Fig. 3a**). Within this (plateau) range of stimulus intensities, a stimulus intensity was chosen that resulted in failures 30–40% of the time. Under these conditions, it is likely that only one fiber is activated. At these stimulus intensities (10–40 μA), 50–100 responses were evoked at 0.2 Hz before drug application, and another ~50 responses were evoked in the presence of bicuculline and strychnine to unmask glutamate components. Successful responses were identified offline by eye. Only those responses whose latencies fell within a 1-ms window were accepted.

Immunohistochemistry. Coronal brainstem slices (400 μm) were prepared as described above and fixed in 4% paraformaldehyde (PFA) for 2 h. Alternatively, rats were deeply anesthetized with isofluorane and then perfused transcardially with phosphate-buffered saline followed by 4% PFA and brains were removed and postfixed overnight. Tissue was cryoprotected in 30% sucrose and then sectioned at 10 μm with a cryostat. For double and triple immunofluorescence labeling, the following primary antibodies were used: rabbit anti–VGLUT1-2 and VGAT (gift of R. Edwards), goat anti–VGLUT1-3 (Chemicon), and mouse anti-SV2 (Iowa Developmental Studies Hybridoma Bank, gift of W. Halfter). Secondary antibodies were conjugated to Cy2, Alexa 488, Cy3 or Cy5 (Jackson; Molecular Probes). Control sections incubated with secondary antibodies alone showed only weak, diffuse background staining. To identify MNTB-LSO axons, MNTB principal cells in 400 μm acute slices (P5–8) were patched with electrodes (3–6 MΩ) containing a 5% solution of Alexa 568 KCl in the standard pipette solution and were held for 20–30 min; slices were then removed to an interface chamber and allowed to recover for 2–3 h before fixation in 4% PFA for 2 h. These slices were resectioned on the cryostat and immunostained for VGLUT3 and SV2. Fluorescence images were acquired in *z*-stacks using a confocal microscope (60× 1.4-NA lens, FV-500, Olympus), with sequential imaging of each channel to minimize bleedthrough between channels. All images shown are of single confocal planes unless stated otherwise. Quantification was performed on images from single confocal planes, with each channel thresholded separately to save the top 10–15% of signal pixels in that channel, using custom Matlab functions. To estimate colocalization across rats and LSOs, the Pearson's correlation coefficient was calculated on the thresholded images for multiple sites in LSOs from different rats and staining runs, and these coefficients were averaged for each pair of labeled proteins. To compare the acquired images with 'random' images with the same spatial statistics, one channel was reflected relative to the other, thus preserving intrachannel spatial statistics while gaining relatively random interchannel correlations. One channel from each image pair was flipped vertically and horizontally, then the correlation coefficient was determined for each flipped image pair; these two values were averaged to obtain the pseudorandom correlation coefficient shown in the white bars.

ACKNOWLEDGMENTS

The authors thank K. Cihil for technical assistance, R. Edwards for VGAT and VGLUT1/2 antibodies, R. Givens for caged glutamate, W. Halfter for SV2 antibodies, and P. Land, S. Shand and S. Watkins for lending histology advice and equipment. We are grateful to E. Aizenman, S. Amara, N.K. Baba, J. Johnson and L. Lillien for comments on an earlier version of the manuscript. This work was supported by grants from the National Institute on Deafness and Other Communication Disorders (K.K., D.C.G.) and the National Institute of Neurological Disorders and Stroke (D.C.G.).

COMPETING INTERESTS STATEMENT

The authors declare that they have no competing financial interests.

Received 7 December; accepted 29 December 2004

Published online at http://www.nature.com/natureneuroscience/

1. Katz, L.C. & Shatz, C.J. Synaptic activity and the construction of cortical circuits. *Science* **274**, 1133–1138 (1996).
2. Hendry, S.H. & Jones, E.G. Reduction in number of immunostained GABAergic neurones in deprived-eye dominance columns of monkey area 17. *Nature* **320**, 750–753 (1986).
3. Otis, T.S., DeKoninck, Y. & Mody, I. Lasting potentiation of inhibition is associated with an increased number of gamma-aminobutyric acid type A receptors activated during miniature inhibitory postsynaptic currents. *Proc. Natl. Acad. Sci. USA* **91**, 7698–7702 (1994).
4. Micheva, K.D. & Beaulieu, C. An anatomical substrate for experience-dependent plasticity of the rat barrel field cortex. *Proc. Natl. Acad. Sci. USA* **92**, 11834–11838 (1995).
5. Korada, S. & Schwartz, I.R. Development of GABA, glycine, and their receptors in the auditory brainstem of gerbil: a light and electron microscopic study. *J. Comp. Neurol.* **409**, 664–681 (1999).
6. Kilman, V., van Rossum, M.C. & Turrigiano, G.G. Activity deprivation reduces miniature IPSC amplitude by decreasing the number of postsynaptic GABA(A) receptors clustered at neurocortical synapses. *J. Neurosci.* **22**, 1328–1337 (2002).
7. Woodin, M.A., Ganguly, K. & Poo, M.M. Coincident pre- and postsynaptic activity modifies GABAergic synapses by postsynaptic changes in Cl^- transporter activity. *Neuron* **39**, 807–820 (2003).
8. Kandler, K. Activity-dependent organization of inhibitory circuits: lessons from the auditory system. *Curr. Opin. Neurobiol.* **14**, 96–104 (2004).
9. Boudreau, J.C. & Tsuchitani, C. Binaural interaction in the cat superior olive S segment. *J. Neurophysiol.* **31**, 442–454 (1968).
10. Moore, M.J. & Caspary, D.M. Strychnine blocks binaural inhibition in lateral superior olivary neurons. *J. Neurosci.* **3**, 237–242 (1983).
11. Kotak, V.C., Korada, S., Schwartz, I.R. & Sanes, D.H. A developmental shift from GABAergic to glycinergic transmission in the central auditory system. *J. Neurosci.* **18**, 4646–4655 (1998).
12. Nabekura, J. *et al.* Developmental switch from GABA to glycine release in single central synaptic terminals. *Nat. Neurosci.* **7**, 17–23 (2004).
13. Kim, G. & Kandler, K. Elimination and strengthening of glycinergic/GABAergic connections during tonotopic map formation. *Nat. Neurosci.* **6**, 282–290 (2003).
14. Sanes, D.H. & Friauf, E. Development and influence of inhibition in the lateral superior olivary nucleus. *Hear. Res.* **147**, 46–58 (2000).
15. Kandler, K. & Friauf, E. Development of glycinergic and glutamatergic synaptic transmission in the auditory brainstem of perinatal rats. *J. Neurosci.* **15**, 6890–6904 (1995).
16. Ahmadi, S. *et al.* Facilitation of spinal NMDA receptor currents by spillover of synaptically released glycine. *Science* **300**, 2094–2097 (2003).
17. Schwartz, I. The superior olivary complex and lateral lemniscal nuclei. in *The Mammalian Auditory Pathway: Neuroanatomy* (eds. Popper, A.N., Fay, R.R. & Webster, D.B.) 117–167 (Springer, New York, 1992).
18. Chatterton, J.E. *et al.* Excitatory glycine receptors containing the NR3 family of NMDA receptor subunits. *Nature* **415**, 793–798 (2002).
19. Kullmann, P.H. & Kandler, K. Glycinergic/GABAergic synapses in the lateral superior olive are excitatory in neonatal C57B1/6J mice. *Brain Res. Dev. Brain Res.* **131**, 143–147 (2001).
20. Lohmann, C., Ehrlich, I. & Friauf, E. Axon regeneration in organotypic slice cultures from the mammalian auditory system is topographic and functional. *J. Neurobiol.* **41**, 596–611 (1999).
21. Stevens, C.F. & Wang, Y. Facilitation and depression at single central synapses. *Neuron* **14**, 795–802 (1995).
22. Aamodt, S.M., Shi, J., Colonnese, M.T., Veras, W. & Constantine-Paton, M. Chronic NMDA exposure accelerates development of GABAergic inhibition in the superior colliculus. *J. Neurophysiol.* **83**, 1580–1591 (2000).
23. Gaiarsa, J.L., Caillard, O. & Ben-Ari, Y. Long-term plasticity at GABAergic and glycinergic synapses: mechanisms and functional significance. *Trends Neurosci.* **25**, 564–570 (2002).
24. Dickson, K.S. & Kind, P.C. NMDA receptors: neural map designers and refiners? *Curr. Biol.* **13**, R920–R922 (2003).
25. Ehrlich, I., Lohrke, S. & Friauf, E. Shift from depolarizing to hyperpolarizing glycine action in rat auditory neurons is due to age-dependent Cl^- regulation. *J. Physiol. (Lond.)* **520**, 121–137 (1999).
26. Fon, E.A. & Edwards, R.H. Molecular mechanisms of neurotransmitter release. *Muscle Nerve* **24**, 581–601 (2001).
27. Helfert, R.H., Bonneau, J.M., Wenthold, R.J. & Altschuler, R.A. GABA and glycine immunoreactivity in the guinea pig superior olivary complex. *Brain Res.* **501**, 269–286 (1989).
28. Bledsoe, S.C. Jr. *et al.* Immunocytochemical and lesion studies support the hypothesis that the projection from the medial nucleus of the trapezoid body to the lateral superior olive is glycinergic. *Brain Res.* **517**, 189–194 (1990).
29. Docherty, M., Bradford, H.F. & Wu, J.Y. Co-release of glutamate and aspartate from cholinergic and GABAergic synaptosomes. *Nature* **330**, 64–66 (1987).
30. O'Malley, D.M. & Masland, R.H. Co-release of acetylcholine and gamma-a2inobutyric acid by a retinal neuron. *Proc. Natl. Acad. Sci. USA* **86**, 3414–3418 (1989).
31. Jonas, P., Bischofberger, J. & Sandkuhler, J. Corelease of two fast neurotransmitters at a central synapse. *Science* **281**, 419–424 (1998).
32. Walker, M.C., Ruiz, A. & Kullmann, D.M. Monosynaptic GABAergic signaling from dentate to CA3 with a pharmacological and physiological profile typical of mossy fiber synapses. *Neuron* **29**, 703–715 (2001).
33. Gutierrez, R. *et al.* Plasticity of the GABAergic phenotype of the 'glutamatergic' granule

cells of the rat dentate gyrus. *J. Neurosci.* **23**, 5594–5598 (2003).
34. Glendenning, K.K., Masterton, R.B., Baker, B.N. & Wenthold, R.J. Acoustic chiasm. III: Nature, distribution, and sources of afferents to the lateral superior olive in the cat. *J. Comp. Neurol.* **310**, 377–400 (1991).
35. Helfert, R.H. *et al.* Patterns of glutamate, glycine, and GABA immunolabeling in four synaptic terminal classes in the lateral superior olive of the guinea pig. *J. Comp. Neurol.* **323**, 305–325 (1992).
36. Kullmann, P.H., Ene, F.A. & Kandler, K. Glycinergic and GABAergic calcium responses in the developing lateral superior olive. *Eur. J. Neurosci.* **15**, 1093–1104 (2002).
37. Ene, F.A., Kullmann, P.H., Gillespie, D.C. & Kandler, K. Glutamatergic calcium responses in the developing lateral superior olive: receptor types and their specific activation by synaptic activity patterns. *J. Neurophysiol.* **90**, 2581–2591 (2003).
38. Ben-Ari, Y., Khazipov, R., Leinekugel, X., Caillard, O. & Gaiarsa, J.L. GABAA, NMDA and AMPA receptors: a developmentally regulated 'menage a trois'. *Trends Neurosci.* **20**, 523–529 (1997).
39. Bellocchio, E.E., Reimer, R.J., Fremeau, R.T. & Edwards, R.H. Uptake of glutamate into synaptic vesicles by an inorganic phosphate transporter. *Science* **289**, 957–960 (2000).
40. Wojcik, S.M. *et al.* An essential role for vesicular glutamate transporter 1 (VGLUT1) in postnatal development and control of quantal size. *Proc. Natl. Acad. Sci. USA* **101**, 7158–7163 (2004).
41. Fremeau, R.T. *et al.* Vesicular glutamate transporters 1 and 2 target to functionally distinct synaptic release sites. *Science* **304**, 1815–1819 (2004).
42. Fremeau, R.T. Jr., Voglmaier, S., Seal, R.P. & Edwards, R.H. VGLUTs define subsets of excitatory neurons and suggest novel roles for glutamate. *Trends Neurosci.* **27**, 98–103 (2004).
43. Harkany, T. *et al.* Endocannabinoid-independent retrograde signaling at inhibitory synapses in layer 2/3 of neocortex: involvement of vesicular glutamate transporter 3. *J. Neurosci.* **24**, 4978–4988 (2004).
44. Lynch, J.W. Molecular structure and function of the glycine receptor chloride channel. *Physiol. Rev.* **84**, 1051–1095 (2004).
45. Malinow, R. AMPA receptor trafficking and long-term potentiation. *Philos. Trans. R. Soc. Lond. B Biol. Sci.* **358**, 707–714 (2003).
46. Furuta, A., Rothstein, J.D. & Martin, L.J. Glutamate transporter protein subtypes are expressed differentially during rat CNS development. *J. Neurosci.* **17**, 8363–8375 (1997).
47. McLean, H.A., Caillard, O., Ben-Ari, Y. & Gaiarsa, J.L. Bidirectional plasticity expressed by GABAergic synapses in the neonatal rat hippocampus. *J. Physiol. (Lond.)* **496**, 471–477 (1996).
48. Morishita, W. & Sastry, B.R. Postsynaptic mechanisms underlying long-term depression of GABAergic transmission in neurons of the deep cerebellar nuclei. *J. Neurophysiol.* **76**, 59–68 (1996).
49. Givens, R.S., Weber, J.F., Jung, A.H. & Park, C.H. New photoprotecting groups: desyl and p-hydroxyphenacyl phosphate and carboxylate esters. *Methods Enzymol.* **291**, 1–29 (1998).